Separation Science and Technology
Publication details, including instructions for authors and subscription information:
http://www.informaworld.com/smpp/title~content=t713708471

Evaluation of Adsorption Characteristics of Malachite Green onto Almond Shell (*Prunus dulcis*)

Duygu Ozdes[a]; Ali Gundogdu[a]; Celal Duran[a]; Hasan Basri Senturk[a]
[a] Department of Chemistry, Faculty of Arts & Sciences, Karadeniz Technical University, Trabzon, Turkey

Online publication date: 15 September 2010

To cite this Article Ozdes, Duygu , Gundogdu, Ali , Duran, Celal and Senturk, Hasan Basri(2010) 'Evaluation of Adsorption Characteristics of Malachite Green onto Almond Shell (*Prunus dulcis*)', Separation Science and Technology, 45: 14, 2076 — 2085
To link to this Article: DOI: 10.1080/01496395.2010.504479
URL: http://dx.doi.org/10.1080/01496395.2010.504479

Separation Science and Technology, 45: 2076–2085, 2010

ISSN: 0149-6395 print/1520-5754 online
DOI: 10.1080/01496395.2010.504479

Taylor & Francis
Taylor & Francis Group

Evaluation of Adsorption Characteristics of Malachite Green onto Almond Shell (*Prunus dulcis*)

Duygu Ozdes, Ali Gundogdu, Celal Duran, and Hasan Basri Senturk
Department of Chemistry, Faculty of Arts & Sciences, Karadeniz Technical University, Trabzon, Turkey

The potential usage of almond shell (*P. dulcis*), which is an agricultural waste product, in the removal of malachite green from aqueous solutions was evaluated with respect to various experimental parameters including contact time, initial malachite green concentration, temperature, adsorbent concentration, etc. The adsorption kinetics of malachite green fitted well the pseudo-second-order kinetic model. The monolayer adsorption capacity of almond shell was found to be 29.0 mg g^{-1}. The adsorption of malachite green onto almond shell increased with raising the temperature. From the experimental results, almond shell could be employed as a low cost and easily available adsorbent for removal of malachite green in wastewater treatment process.

Keywords adsorption; almond shell; kinetic; malachite green; removal; thermodynamic

INTRODUCTION

Synthetic dyestuffs are extensively used in many industries such as textiles, paper, tannery, food, rubber, plastics, cosmetics, printings, etc. to color their products. The presence of dyes and pigments in water is highly visible and undesirable even at low concentrations (1). The dyes, in industrial effluents not only affect the aesthetic merits, they can cause problems in several ways: the presence of dyes in natural streams reduces light penetration, retards the photosynthetic activity, inhibits the growth of biota, and also has a tendency to chelate metal ions that produce micro-toxicity to fish and other organisms (2); dyes can have acute or chronic effects on exposed organisms depending on the exposure time and concentration (3); as a result of direct contact, inhalation or ingestion of dyes can cause eye burns, rapid or difficult breathing, nausea, and vomiting, etc. in humans (4).

Malachite Green (MG, Fig. 1), is a cationic dye (Color Index (CI): 42000, chemical formula: $C_{23}H_{25}ClN_2$, formula weight (FW): 364.9 g mol^{-1}, and absorbance maximum (λ_{max}): 617 nm) which is widely used to color cotton, jute, silk, wool, leather and also extensively used in the fish farming industry as fungicide, ectoparasiticide, and disinfectant all over the world (5). The MG, an *N*-methylated diaminotriphenylmethane dye, exhibits carcinogenic, genotoxic, mutagenic, and teratogenic properties due to its nitrogen composition. The discharge of MG into receiving streams damages the aquatic life by causing detrimental effects in liver, gall, kidney, intestine, gonads, and pituitary gonadotrophic cells. In humans, as a result of inhalation it may cause irritation to the respiratory tract and also causes irritation to the gastrointestinal tract upon ingestion. It is also highly toxic to mammalian cells and acts as a tumor enhancing agent (6–8). For these reasons the removal of MG and other toxic dyestuffs from waters and wastewaters is an important application in terms of protection of human health, aquatic life, and environment.

Various attempts have been made for the treatment of dye-containing wastewaters including photodegradation, flocculation, chemical and biological oxidation, ozonation, aerobic and anaerobic microbial degradation, chemical precipitation, ion exchange, filtration, and membrane processes (3,6). Nevertheless some of these techniques have significant disadvantages such as incomplete dye removal, high reagent and energy necessity, low selectivity, and generation of secondary wastes that are difficult to be disposed off. For example, among the conventional methods, the precipitation method followed by coagulation is particularly credible for the removal of dyes from water. But this process requires large settling tanks for precipitation of large volumes of sludge and also subsequent treatment is needed. Although membrane filtration is a proven way to remove dyes, its high cost limits the use of this method. Otherwise, the removal of dyes by adsorption is considered as one of the most powerful separation and purification methods due to its high efficiency, easy handling, high selectivity, and lower operating cost (9). In order to enhance the efficiency of the adsorption process, it is necessary to develop new adsorbents, which are economical, easily available, and have strong affinity and high loading capacity (10).

Received 28 September 2009; accepted 10 May 2010.
Address correspondence to Celal Duran, Department of Chemistry, Faculty of Arts & Sciences, Karadeniz Technical University, Trabzon 61080, Turkey. Tel.: +90 462 3772491; Fax: +90 462 3253196. E-mail: cduran@ktu.edu.tr

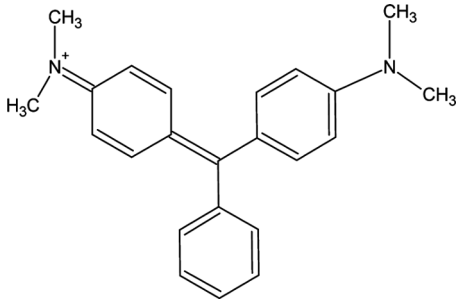

FIG. 1. Molecular structure of MG.

It is well known that the adsorption process is strongly affected by the chemistry and surface morphology of the adsorbent. Although the activated carbon is a most widely used adsorbent due to its large surface area, micro-porous structure, and high adsorption capacity, its high cost, low selectivity, and difficulties in recovering of activated carbon particles from treated water, limit its use as an adsorbent (11). The agricultural and forestry waste products represent unused resources and also they are widely available and environmentally friendly so they have a great potential to be used as adsorbents. A number of low cost agricultural materials including Arundo donax root (12), sugar cane dust (13), wheat bran (14), waste apricot (15), de-ioled soya (16), etc. have been used for the removal of MG from waters and wastewaters. The almond shell (AS) which is widely distributed in Turkey, was selected as an adsorbent for the removal of MG from aqueous solutions. The annual production of AS is an average of 30.000 tons in Turkey (17). The AS (*P. dulcis*) is available as an agricultural waste product for which no important industrial use has been developed so it is one of the most abundant, effective, and cheap material. The AS was used in this study without any physical or chemical pretreatment. The utilization of AS without previous activation treatment is another feature of this study with respect to a decrease in the cost of the adsorption process. Ardejani et al. have proposed an adsorption process to remove Direct Red 80 dye from aqueous solution by using AS (18). Furthermore, the AS and its activated carbon have been used for metal removal studies by previous researchers, such as Bulut and Tez who have evaluated the adsorption behavior of Ni(II), Cd(II), and Pb(II) from aqueous solutions by shells of hazelnut and almond (19) and the adsorption of copper (Cu), zinc (Zn), lead (Pb), and cadmium (Cd) that exist in industrial wastewater onto the activated carbon produced from nutshells of walnut, hazelnut, pistachio, almond, and apricot stone has been investigated by Kazemipour et al. (20). All these researches indicated that the AS and its activated carbon can be effectively used for dye and metal removal processes.

The objective of the present study was to evaluate the potential usage of AS as a low cost adsorbent in the removal of one of the highly toxic dye, MG, from aqueous solutions. The effects of important experimental parameters such as contact time, initial MG concentration, adsorbent concentration, ionic strength, etc. were studied. The adsorption mechanisms of MG onto AS were evaluated in terms of thermodynamics and kinetics. The adsorption isotherms were described by using the Langmuir and Freundlich models.

MATERIALS AND METHODS

Preparation and Characterization of Adsorbent

The AS was collected from a local market in Turkey, and it was washed with deionized water several times to remove surface impurities, then dried in an oven (Nüve FN 400) at 40°C for 4 days. The dried AS samples were ground in a blender and sieved to obtain a particle size of $<150\,\mu m$, and stored in glass containers to be used for adsorption experiments. No other physical or chemical treatments were carried out prior to the adsorption experiments.

The FTIR spectra of the natural AS and MG loaded AS were obtained to determine the surface functional groups by using Perkin Elmer 1600 FTIR spectrophotometer in the range of 4000–400 cm^{-1}.

Adsorption Experiments

All chemicals used in this work were of analytical reagent grade and were used without further purification. Deionized water was used for all dilutions. All glassware and plastics were soaked in 10% (v/v) nitric acid solution for one day before use, and then cleaned repeatedly with deionized water. The effect of pH on the adsorption capacity was not carried out since the addition of dilute acids and/or bases caused the color change of MG (21). Hence the adsorption studies were conducted at natural pH of MG (depending on the MG concentration in the pH range of 3.0 and 4.5). The adsorption of MG onto AS was performed through a batch process. For adsorption experiments, 10 mL of MG solution in the concentration range of 70–1150 mg L^{-1} was transferred into a polyethylene centrifuge tube. Then 100 mg of AS (10 g L^{-1} suspension) was added to the solution, and then the mixture was agitated on a mechanical shaker (Edmund Bühler GmbH) at 400 rpm. After reaching equilibrium, the suspension was filtered through 0.45 μm of nitrocellulose membrane (Sartorius Stedim Biotech. GmbH), and the filtrate was analyzed for residual MG concentration using a double beam UV-Vis spectrophotometer (Unicam UV-2 Spectrophotometer) at a wavelength of 620 nm. All experiments were conducted in triplicate, and the averages of the results were submitted for data analysis. In the presented adsorption method, relative standard deviation (RSD) was obtained after analyzing a series of 10 replicates by contacting 10 mL of 100 mg L^{-1} of MG solutions with 10 g L^{-1} of

AS suspensions under the optimum experimental conditions. From the results, RSD was found to be lower than 1.2%. The detection limit, defined as the concentration equivalent to three times the standard deviation of 10 replicate measurements of blank samples, was found to be $0.32\,mg\,L^{-1}$.

The amount of the MG adsorbed by the AS was calculated as the following equations;

$$\text{Removal } (\%) = \frac{C_o - C_e}{C_o} \times 100 \quad (1)$$

$$Q_e = \frac{(C_o - C_e)V}{m_s} \quad (2)$$

C_o ($mg\,L^{-1}$) is the initial concentration of MG solution, C_e ($mg\,L^{-1}$) is the equilibrium concentration of MG in aqueous solution, V (L) is the volume of solution, m_s (g) is the mass of the AS and Q_e ($mg\,g^{-1}$) is the calculated MG adsorption amount onto 1.0 gram of AS.

RESULTS AND DISCUSSION

FTIR Studies

The physical and chemical properties of AS were determined by the previous researchers (19). The FTIR spectra of natural AS and MG loaded AS were depicted in Figs. 2(a) and 2(b) in order to compare the differences among them. The positions of the peaks obtained from FTIR spectra of AS and MG loaded AS were approximately similar but it is important to notice that the band intensities decreased from 56 to 46% in the FTIR spectrum of MG loaded AS. The FTIR measurements show the presence of the following groups: O–H ($3400\,cm^{-1}$; stretch vibration), C–H aromatic and aliphatic ($2930\,cm^{-1}$; stretch vibration), C=O ($1740\,cm^{-1}$; stretch vibration), C=C aromatic (1608 and $1505\,cm^{-1}$; stretch vibration), C–H (1465 and $1378\,cm^{-1}$; deformation vibration), and C–O ($1040\,cm^{-1}$; stretch vibration). Similar results were obtained by Estevinho et al. (22) with pentachlorophenol adsorption by AS residues, and by Ardejani et al. (18) with Direct Red 80 dye adsorption from aqueous solution onto almond shells.

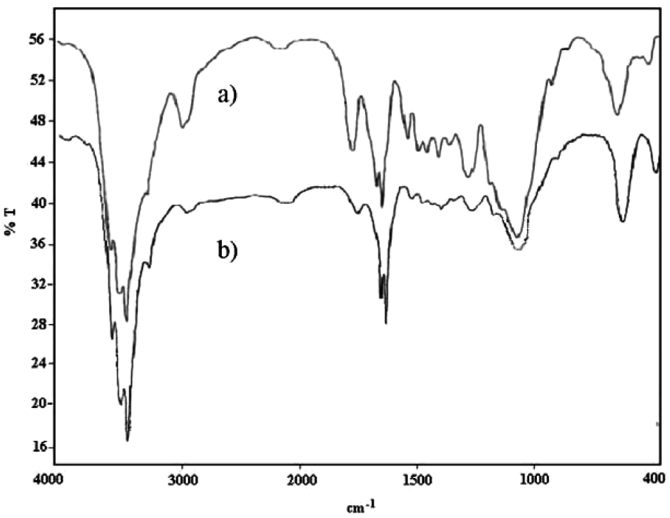

FIG. 2. FTIR spectra of a) AS b) MG loaded AS.

Effect of Contact Time and Adsorption Kinetics

The time-dependent behavior of MG adsorption was studied by contacting different concentrations of MG in the range of 100–1000 $mg\,L^{-1}$ with 10 $g\,L^{-1}$ of AS suspensions in the test tubes. The tubes were taken at the different contact times in the range of 1–480 min and immediately filtered through 0.45 μm of nitrocellulose membrane. The data showed that the adsorption of MG was rapid at the initial stage of contact time and thereafter it continued at a slower rate, and finally reached saturation for all initial dye concentrations (Fig. 3(a)). This can be explained by the fact that, at the beginning of the adsorption the active adsorption sites on the AS surface were open so MG interacted easily with these sites but as the time proceeded the accumulation of MG particles on the surface of AS lead to decrease the adsorption rate (23). The adsorption reached equilibrium within about 60 min for initial dye concentration of $100\,mg\,L^{-1}$, 120 min for initial dye concentration of $400\,mg\,L^{-1}$ and 180 min for initial dye concentrations of 600 and $1000\,mg\,L^{-1}$. The faster adsorption of MG at lower concentrations was an indication that MG adsorption occurred mainly on the surface of AS. As the MG concentration increased, the adsorption process probably occurred in three stages: the first stage was fast as a result of rapid attachment of MG to the surface of AS, the second stage was slower maybe because the adsorption took place in the pores of AS as a result of intraparticle diffusion, and in the third stage the adsorption process reached the equilibrium (24,25).

In order to investigate the adsorption kinetics of MG onto AS, three different kinetic models, which are pseudo-first-order, pseudo-second-order, and intraparticle diffusion models have been used to fit the experimental data obtained from batch removal experiments.

The pseudo-first-order Lagergren model is expressed as (26);

$$\frac{d_Q}{d_t} = k_1(Q_e - Q_t) \quad (3)$$

where Q_e ($mg\,g^{-1}$) and Q_t ($mg\,g^{-1}$) are the amounts of the MG adsorbed on the AS at equilibrium and at any time t, respectively; and k_1 (min^{-1}) is the rate constant of the first-order adsorption.

After integration and applying boundary conditions $Q_t = 0$ at $t = 0$ and $Q_t = Q_t$ at $t = t$ the integrated form of

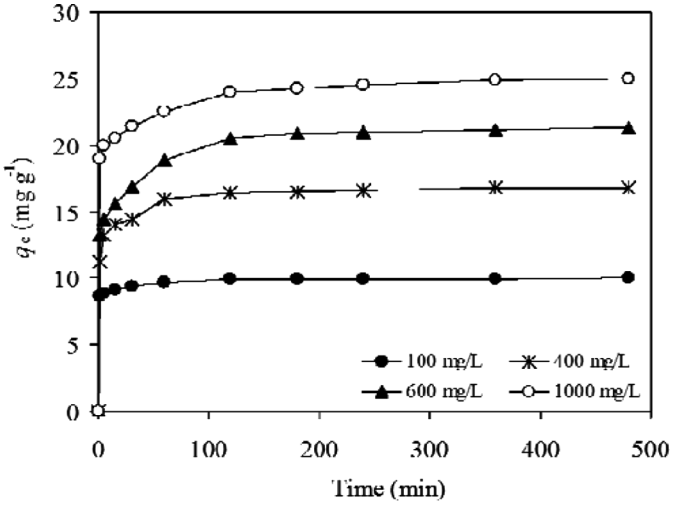

(a)

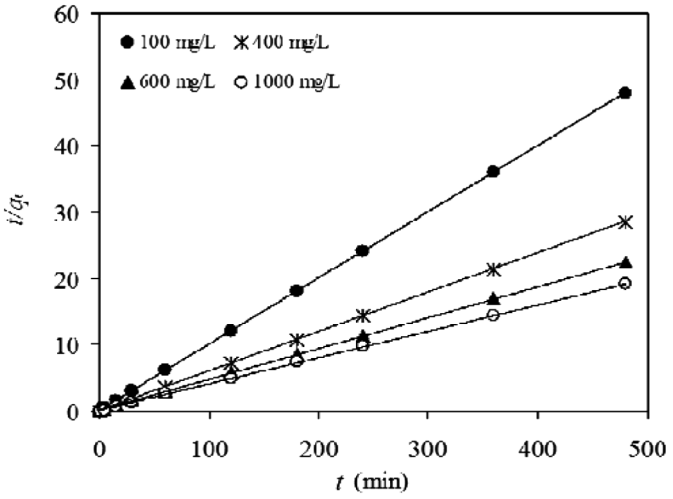

(b)

FIG. 3. (a) Effect of contact time on the MG uptake, (b) Pseudo-second-order kinetic model.

Eq. (3) becomes;

$$\ln(Q_e - Q_t) = \ln Q_e - k_1 t \tag{4}$$

The value of k_1 and Q_e can be obtained from the slope and intercept of the linear plot of $\ln(Q_e - Q_t)$ versus t, respectively.

The second-order-kinetic model, which is based on the assumption that the adsorption follows a chemisorption process, can be written as the following form (27);

$$\frac{d_Q}{d_t} = k_2(Q_e - Q_t)^2 \tag{5}$$

where k_2 (g mg^{-1} min^{-1}) is the rate constant of the second-order equation; Q_e (mg g^{-1}) is the maximum adsorption capacity; Q_t (mg g^{-1}) is the amount of adsorption at time t (min).

After definite integration by applying the conditions $Q_t = 0$ at $t = 0$ and $Q_t = Q_t$ at $t = t$ the Eq. (5) becomes the following;

$$\frac{t}{Q_t} = \frac{1}{k_2 Q_e^2} + \frac{t}{Q_e} \tag{6}$$

The value of Q_e and k_2 can be obtained from the slope and intercept of the linear plot of t/Q_t versus t, respectively.

The intraparticle diffusion equation is expressed as (28);

$$Q_t = k_{id} t^{1/2} + c \tag{7}$$

where Q_t (mg g^{-1}) is the amount of adsorption at time t (min) and k_{id} (mg g^{-1} min$^{-1/2}$) is the rate constant of intraparticle diffusion. The values of k_{id} and c can be determined from the slope and intercept of the plot of Q_t versus $t^{1/2}$, respectively.

The pseudo-first-order rate constants (k_1) and theoretical equilibrium adsorption capacities ($Q_{e\ cal}$), calculated from linear plots of $\ln(Q_e - Q_t)$ versus t for all studied initial MG concentrations, were given along with the correlation coefficients (R^2) in Table 1. The obtained R^2 values were relatively small and the calculated Q_e values ($Q_{e\ cal}$) were much lower than the experimental values of Q_e ($Q_{e\ exp}$). These observations suggested that the pseudo-first-order model is not suitable for modeling the adsorption of MG onto AS.

The linear plots of t/Q_t versus t for the pseudo-second-order kinetic model were shown in Fig. 3(b) and the rate constants k_2 and the values of $Q_{e\ cal}$ along with the corresponding R^2 values for all studied initial MG concentrations were presented in Table 1.

The intraparticle rate constant (k_{id}) and c parameters, obtained from the plots of Q_t versus $t^{1/2}$ for the intraparticle diffusion model, were given in Table 1. The values of c obtained from the intraparticle diffusion model was not zero and the R^2 values were not satisfactory (in the range of 0.29–0.42), indicating that the intraparticle diffusion may not be the controlling factor in determining the kinetics of the process.

Since the R^2 values were closer to unity for the pseudo-second-order kinetic model for all studied initial MG concentrations and $Q_{e\ cal}$ values agreed reasonably well with the experimental data than those for the other kinetic models, the adsorption kinetics can be represented by the pseudo-second-order kinetic model. These observations implied that the adsorption of MG onto AS belongs to the pseudo-second-order kinetic model, based on the assumption that the rate-limiting step may be chemical adsorption or chemisorption.

TABLE 1
Parameters of pseudo-first-order, pseudo-second-order, and intraparticle diffusion model

		Pseudo-first-order			Pseudo-second-order			Intraparticle diffusion model		
C_o (mg/L)	$Q_{e\ exp}$ (mg g^{-1})	$Q_{e\ cal}$ (mg g^{-1})	k_1 (min^{-1})	R^2	$Q_{e\ cal}$ (mg g^{-1})	k_2 (g mg^{-1} min^{-1})	R^2	k_{id} (mg g^{-1} min$^{-1/2}$)	C (mg g^{-1})	R^2
100	10.0	1.3	−0.0127	0.77	10.01	0.089	0.999	0.208	6.76	0.287
400	16.8	4.2	−0.0135	0.87	16.84	0.024	0.999	0.439	9.78	0.446
600	22.3	7.5	−0.0134	0.97	21.41	0.011	0.998	0.630	10.93	0.565
1000	25.0	6.7	−0.0120	0.90	25.06	0.012	0.999	0.615	14.91	0.417

Effect of Initial MG Concentration and Adsorption Isotherms

The effect of initial MG concentration on the adsorption process was investigated at a constant AS concentration (10 g L^{-1}) and different initial MG concentrations in the range of 70–1150 mg L^{-1}. The equilibrium concentration of MG increased from 5.0 to 25.0 mg g^{-1} whereas the adsorption percentage decreased from 71.6 to 21.5% with increasing the initial MG concentration from 70 to 1150 mg L^{-1} (Fig. 4). The higher initial concentration of MG provides an important driving force to overcome mass transfer resistance for MG transport between the solution and the surface of the AS. Furthermore, increasing the initial MG concentration increases the number of collisions between MG ions and AS, which enhances the adsorption amount. On the other hand, at a constant AS concentration, the decrease in the adsorption percentage was probably due to the saturation of the active binding sites on the AS at higher MG concentrations, hence MG present in solution cannot interact with these sites easily (29,30).

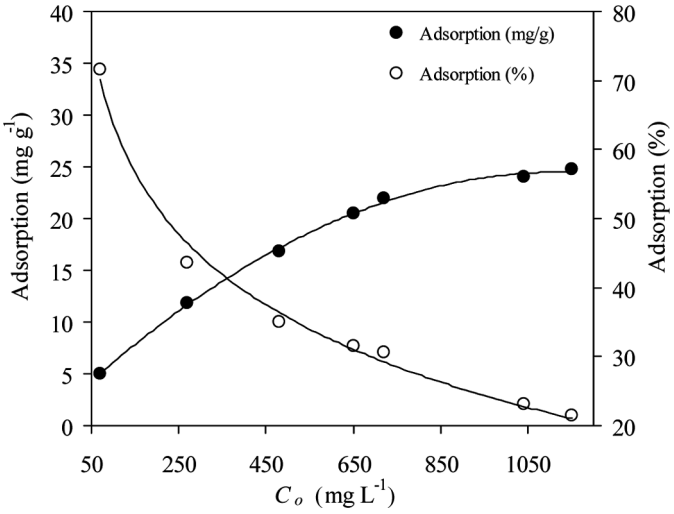

FIG. 4. Effect of initial MG concentration on MG uptake (AS conc.: 10 g L^{-1}).

Two commonly used isotherm models, Langmuir and Freundlich, were applied to the experimental data in order to design the adsorption system and evaluate the applicability of the adsorption process (13).

The Langmuir isotherm is valid for the monolayer adsorption on a homogeneous surface. It is expressed by (31);

$$Q_e = \frac{bQ_{max}Ce}{1 + bQ_{max}} \tag{8}$$

where Q_e (mg g^{-1}) is the amount of the dye adsorbed per unit mass of adsorbent, C_e (mg L^{-1}) is the equilibrium dye concentration in the solution, Q_{max} (mg g^{-1}) is the Langmuir constant related the maximum monolayer sorption capacity and b (L mg^{-1}) is the constant related to the free energy or net enthalpy of adsorption. The Langmuir model in linear form;

$$\frac{C_e}{Q_e} = \frac{C_e}{Q_{max}} + \frac{1}{bQ_{max}} \tag{9}$$

The linear plot of C_e/Q_e versus C_e (Fig. 5(a)) suggested the applicability of the Langmuir isotherm model for the adsorption of MG onto AS. The values of Q_{max} and b, obtained from the slope and intercept of the plot, were found to be 29.0 mg g^{-1} and 0.0057 L mg^{-1}, respectively, with a correlation coefficient (R^2) of 0.982. The Q_{max} values of other adsorbents for the adsorption of MG by hen feathers (32), iron humate (33), Arundo donax root (12), bentonite (34), sugar cane dust (13) were 26.1, 19.2, 8.69, 7.72, and 4.88 mg g^{-1}, respectively.

The essential characteristics of the Langmuir isotherm model can be described by means of 'R_L', a dimensionless constant referred to as the separation factor or equilibrium parameter. R_L can be calculated using the following equation (35);

$$R_L = \frac{1}{1 + bC_o} \tag{10}$$

where C_o (mg L^{-1}) is the initial concentration of dye and b (L mg^{-1}) is the Langmuir constant described above. R_L

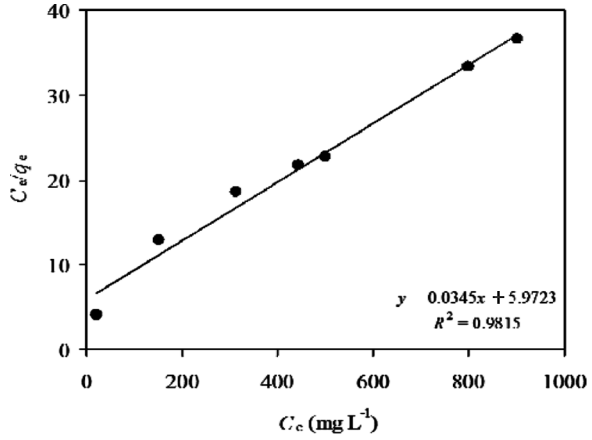

(a)

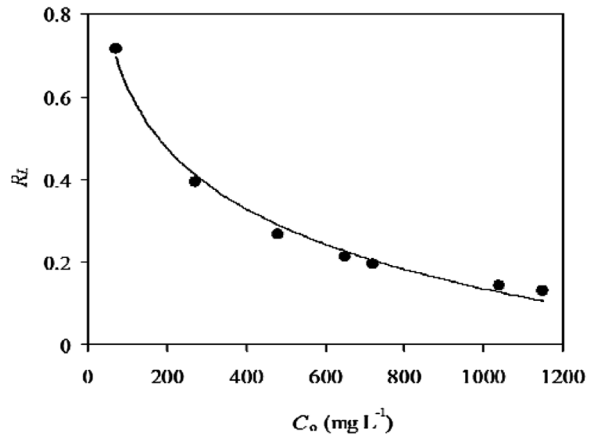

(b)

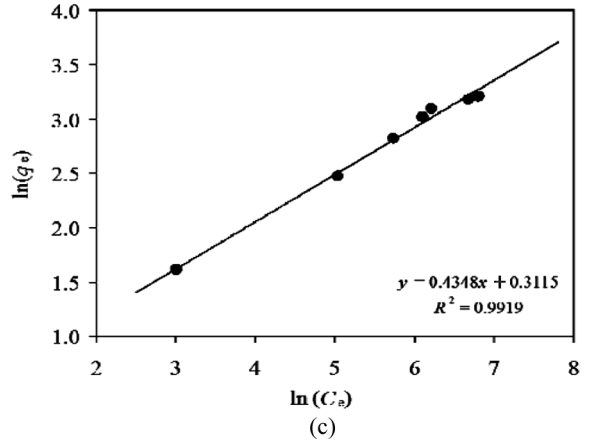

(c)

FIG. 5. (a) Langmuir isotherm model, (b) Variation of R_L values with initial MG concentrations, (c) Freundlich isotherm model.

value referred the shape of the adsorption to be either favorable ($0 < R_L < 1$), unfavorable ($R_L > 1$), linear ($R_L = 1$), or irreversible ($R_L = 0$). The R_L values ranged from 0.715 to 0.132 between 70 and 1150 mg L^{-1} of initial MG concentration indicated that favorable adsorption occurred for MG (Fig. 5(b)).

The Freundlich isotherm model is based on the adsorption on heterogeneous surfaces and presented by the following equation (36);

$$Q_e = K_f C_e^{1/n} \tag{11}$$

where K_f (mg g^{-1}) is the constant related to the adsorption capacity and n is the empirical parameter related to the intensity of adsorption. The value of n varies with the heterogeneity of the adsorbent and for favorable adsorption process the value of n should be less than 10 and higher than unity. The Freundlich model in linear form;

$$\ln Q_e = \ln K_f + \frac{1}{n} \ln C_e \tag{12}$$

The values of Freundlich constants, K_f and n, obtained from the linear plot of $\ln Q_e$ versus $\ln C_e$ (Fig. 5(c)), were found to be 1.365 mg g^{-1} and 2.30 respectively, with a correlation coefficient (R^2) of 0.992. The value of n was found to be larger than unity and indicated that the adsorption process was favorable under studied conditions.

These observations indicated that the adsorption pattern of MG onto AS was well fitted with both the Langmuir and Freundlich isotherm models. This may be due to both homogeneous and heterogeneous distribution of active sites on the surface of the AS.

Effect of Adsorbent Concentration

The effect of AS concentration on the uptake of MG from aqueous solution was studied by using initial MG concentration of 360 mg L^{-1} and varying AS concentration from 1.0 to 20.0 g L^{-1}. As the AS concentration increased from 1.0 to 20.0 g L^{-1}, the equilibrium adsorption capacity of AS decreased from 34.0 to 17.1 mg g^{-1}, whereas, the MG removal efficiency increased from 9.3 to 94.0% (Fig. 6). The increase in the removal efficiency could be attributed to increased availability of more active adsorption sites with the increase in AS concentration. The decrease in the amount of MG adsorbed per unit mass of AS with increase in AS concentration could be explained by the fact that some adsorption sites remained unsaturated during the adsorption process and also overlapping or aggregation of adsorption sites resulting in decrease in the total available surface area of AS (13,37).

Effect of Temperature and Thermodynamic Parameters

Temperature has a significant impact on the adsorption capacity depending on the structure and surface functional groups of an adsorbent (38). In order to evaluate the effect of temperature on the uptake of MG, the adsorption experiments were conducted in the temperature range of 0–40°C with AS concentration of 10 g L^{-1} and initial MG concentration of 100 mg L^{-1}. The adsorption of MG onto

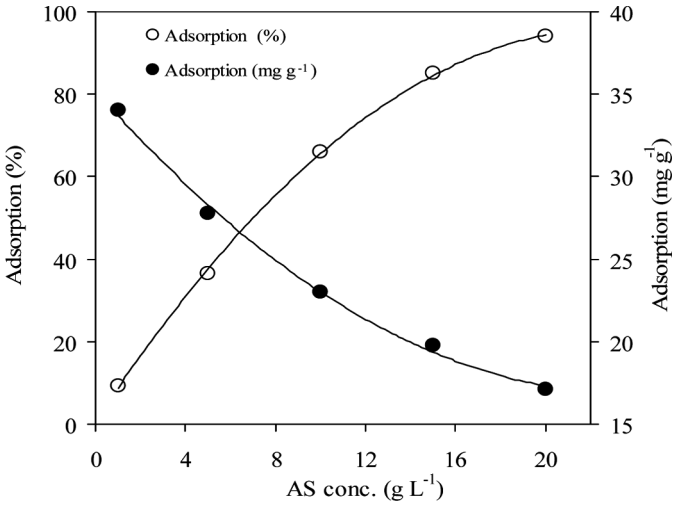

FIG. 6. Effect of AS concentration on MG uptake (initial MG conc.: 360 mg L^{-1}, contact time: 2 h).

AS increased from 8.7 mg g^{-1} (62% removal) to 12.0 mg g^{-1} (85% removal) when the temperature increased from 0 to 40°C (Fig. 7(a)), which is indicative of the endothermic process in nature so the MG uptake by adsorption onto AS favors at higher temperature.

The thermodynamic parameters including Gibbs free energy change (ΔG), enthalpy (ΔH), and entropy (ΔS) were calculated from the following equation (39);

$$\Delta G = -RT \ln K_d \tag{13}$$

where R is the universal gas constant (8.314 J mol^{-1} K^{-1}), T is the temperature (K), and K_d is the distribution coefficient. The K_d value was calculated using the following equation;

$$K_d = \frac{Q_e}{C_e} \tag{14}$$

where Q_e and C_e are the equilibrium concentration of MG on adsorbent (mg L^{-1}) and in the solution (mg L^{-1}), respectively. The enthalpy (ΔH) and entropy change (ΔS) of adsorption were estimated from the following equation;

$$\Delta G = \Delta H - T\Delta S \tag{15}$$

These equations can be written as;

$$\ln K_d = \frac{\Delta S}{R} - \frac{\Delta H}{RT} \tag{16}$$

The ΔH and ΔS were obtained from the slope and intercept of the plot between $\ln K_d$ versus $1/T$, respectively (Fig. 7(b)). The values of K_d, ΔH, ΔS, and ΔG are presented in Table 2. The negative values of ΔG, in the temperature range of 0–40°C, suggested the feasibility of the process and spontaneous nature of the adsorption of MG onto AS while the positive value of ΔH indicated the endothermic nature of adsorption which was also

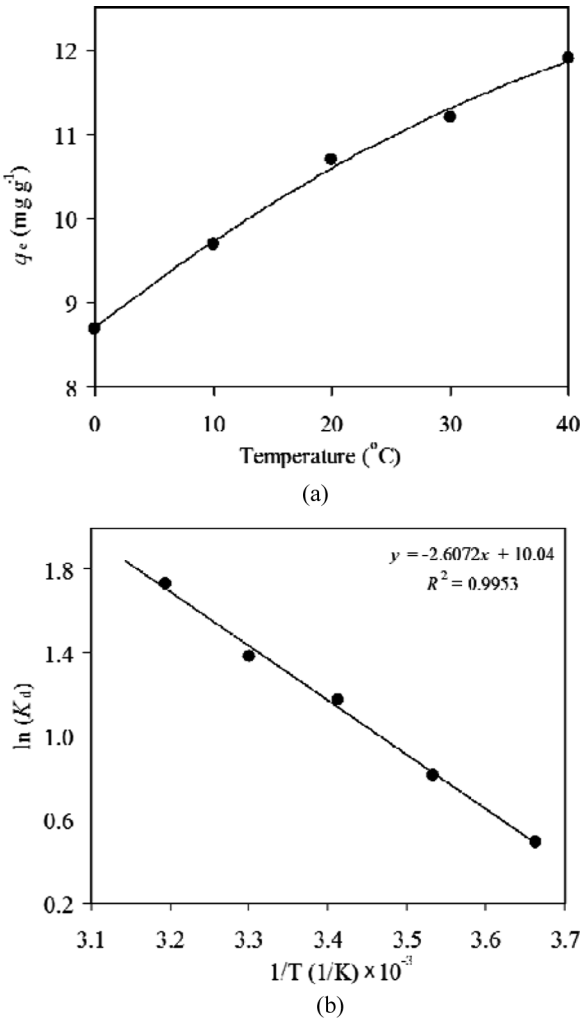

FIG. 7. (a) Effect of temperature on MG uptake, (b) The plot between $\ln K_d$ versus $1/T$ for obtaining the thermodynamic parameters (initial MG conc.: 100 mg L^{-1}, AS conc.: 10 g L^{-1}, contact time: 1 h).

TABLE 2
Thermodynamic parameters of the MG adsorption onto AS at different temperatures

T (°C)	K_d	ΔG (kJ mol^{-1})	ΔS (J mol^{-1} K^{-1})[a]	ΔH (kJ mol^{-1})[a]
0	1.64	−1.12		
10	2.26	−1.91		
20	3.24	−2.87	83.47	21.67
30	4.00	−3.49		
40	5.67	−4.51		

[a]Measured between 273 and 313 K.

supported by the increase in value of MG uptake of the adsorbent with the rise in temperature. The positive value of ΔS implied the increased randomness at the solid-solution interface during the adsorption of MG onto AS and also reflected the affinity of the AS material towards MG.

Effect of Ionic Strength

The wastewaters released into the environment from different industries may contain various types of salts besides dyestuffs and that is why the effect of ionic strength upon the uptake of MG was studied by adding KCl, Na_2SO_4, and $NaNO_3$ solutions individually, in 182 mg L^{-1} of MG solutions, containing 10 g L^{-1} of AS, and the present adsorption process was applied to these solutions. The adsorption amount of MG decreased with increasing of KCl and $NaNO_3$ concentrations in the solution (Fig. 8). This can be explained by the fact that the cations (K^+ and Na^+) from the salts compete with MG ions for the active adsorption sites of AS so the electrostatic interactions between MG and surface functional groups of AS were impeded in the presence of ionic strength. On the other hand, the Na_2SO_4 salt causes an increase in the degree of dissociation of the MG molecules by facilitating the protonation. The adsorbed amount of MG increased as the dissociated MG ions left free for binding electrostatically onto the oppositely charged AS surface (40,41).

Reuse of the AS without Regeneration

The adsorption experiments were performed to test the reusability of MG loaded AS without regeneration by contacting initial MG concentration of 170 mg L^{-1} with 10 g L^{-1} of AS suspension. After shaking for 2 hours, the MG loaded AS was separated, dried in air for one day, and then treated with another 170 mg L^{-1} MG solution. The process was repeated five times. The largest amount of MG adsorbed (69% removal) was with fresh AS (first cycle), and in each of its subsequent loading the adsorption capacity of AS was decreased. After cycles 2, 3, 4, and 5, the newly adsorbed amount of MG were 7.4 mg g^{-1} (43.5% removal), 3.2 mg g^{-1} (19% removal), 1.6 mg g^{-1} (9.4% removal) and 0.4 mg g^{-1} (2.3% removal), respectively. The results suggested that already used AS can be applied for MG adsorption at least four times without regeneration. Similar results were reported in the literature by Ozdes et al. (42).

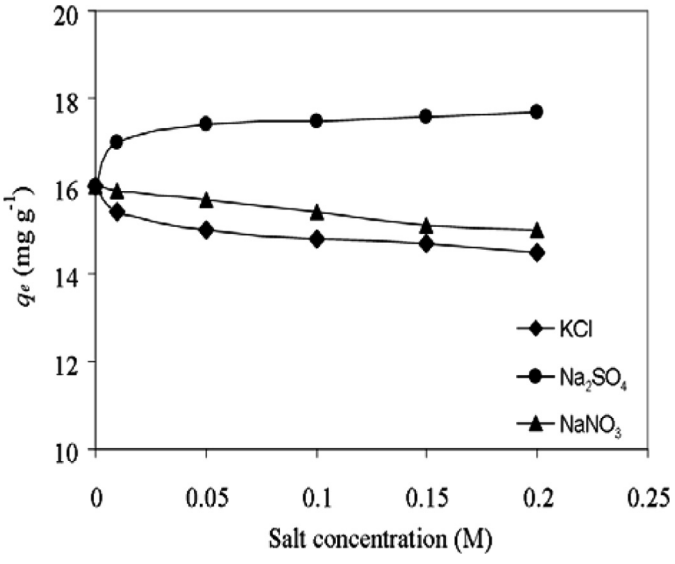

FIG. 8. Effect of ionic strength on the MG uptake (initial MG conc.: 182 mg L^{-1} AS conc.: 10 g L^{-1}, contact time: 2 h).

Desorption of MG

The desorption process enables the recovery of the dyes from wastewater and regeneration of the adsorbent which keeps the adsorption process costs down (43). Desorption of MG from the loaded AS was also studied in a batch system and 20% acetone, 20% ethanol solutions, and deionized water were tried as desorbing agents since they all are considered as cheap and non-polluting solvents. For desorption experiments, 10 g L^{-1} of AS suspension was equilibrated with 10 mL of 100 mg L^{-1} MG solution. After reaching the equilibrium the AS was separated by filtration, then the equilibrium concentration of MG in the filtrate was determined by UV-Vis spectrometry. The MG loaded AS was washed with deionized water three times and then dried in air for one day. The loaded adsorbent was treated with 10 mL of 20% acetone and 20% ethanol solutions and deionized water individually by agitating at 400 rpm for 1 hour. Among the desorbing solutions used in the present study, 20% ethanol solution was identified as the best eluent as it has 96% desorption efficiency. On the other hand, 20% acetone solution has 76.5% desorption efficiency. Desorption of MG could not be achieved by using deionized water (4.1% desorption efficiency).

CONCLUSIONS

Adsorptive removal of a toxic cationic dyestuff, MG, onto natural AS was investigated. The utilization of AS may be the main advantage of the present study because it is an agricultural waste material, so this waste represents unused resources and also presents serious disposal problems. Another feature of this study was to use the AS without any previous activation treatment which decreases the adsorption costs. Furthermore, the AS is considered as one of the most promising adsorbents for dye uptake due to its low cost, easy availability, high dye uptake capacity, and reusability in repeated cycles.

Adsorption characteristics of MG onto AS were found to be influenced by several experimental parameters. The kinetics of MG adsorption onto AS followed by

pseudo-second-order model for all investigated initial MG concentrations. The linear Langmuir and Freundlich isotherm models were used to represent the experimental data, and both models fitted well. The monolayer adsorption capacity of AS was found to be 29.0 mg g^{-1} by using the Langmuir model equations. By comparing the other adsorption processes in the literature which are performed by using different adsorbents, the obtained Q_{max} value clearly indicated that the AS-based adsorption process presents an efficient and low-cost technology for the treatment of MG-containing wastewaters. The negative value of ΔG and the positive value ΔS showed that the adsorption of MG onto AS was feasible and spontaneous. The positive value of ΔH confirmed the endothermic nature of adsorption.

On the basis of all the results, it can be concluded that natural AS can be used effectively for the removal of MG from aqueous solutions using the present adsorption process.

ACKNOWLEDGEMENTS

Authors wish to thank the Unit of the Scientific Research Projects of Karadeniz Technical University (Project No: 2008.111.002.1) for the financial support.

REFERENCES

1. Sun, X.F.; Wang, S.G.; Liu, X.W.; Gong, W.X.; Bao, N.; Gao, B.Y.; Zhang, H.Y. (2008) Biosorption of malachite green from aqueous solutions onto aerobic granules: Kinetic and equilibrium studies. *Bioresour. Technol.*, 99 (9): 3475–3483.
2. Hamdaoui, O. (2006) Dynamic sorption of methylene blue by cedar sawdust and crushed brick in fixed bed columns. *J. Hazard. Mater.*, 38 (2): 293–303.
3. Wang, X.S.; Zhou, Y.; Jiang, Y.; Sun, C. (2008) The removal of basic dyes from aqueous solutions using agricultural by-products. *J. Hazard. Mater.*, 157 (2–3): 374–385.
4. Hameed, B.H.; Din, A.T.M.; Ahmad, A.L. (2007) Adsorption of methylene blue onto bamboo-based activated carbon: Kinetics and equilibrium studies. *J. Hazard. Mater.*, 141 (3): 819–825.
5. Gong, R.; Jin, Y.; Chen, F.; Chen, J.; Liu, Z. (2006) Enhanced malachite green removal from aqueous solution by citric acid modified rice straw. *J. Hazard. Mater.*, 137 (2): 865–870.
6. Bulut, E.; Ozacar, M.; Sengil, I.A. (2008) Adsorption of malachite green onto bentonite: Equilibrium and kinetic studies and process design. *Micropor. Mesopor. Mater.*, 115 (3): 234–246.
7. Srivastava, S.; Sinha, R.; Roy, D. (2004) Toxicological effects of malachite green. *Aquat. Toxicol.*, 66 (3): 319.
8. Chen, J.; Mao, J.; Mo, X.; Hang, J.; Yang, M. (2009) Study of adsorption behavior of malachite green on polyethylene glycol micelles in cloud point extraction procedure. *Colloid Surface A*, 345 (1–3): 231–236.
9. Ahmad, R.; Mondal, P.K. (2009) Application of acid treated almond peel for removal and recovery of brilliant green from industrial wastewater by column operation. *Journal of Separation Science and Technology*, 44 (7): 1638–1655.
10. Rajeshkannan, R.; Rajamohan, N.; Rajasımman, M. (2009) Removal of malachite green from aqueous solution by sorption on hydrilla verticillata biomass using response surface methodology. *Front. Chem. Eng. China*, 3 (2): 146–154.
11. Rao, M.M.; Ramesh, A.; Rao, G.P.C.; Seshaiah, K. (2006) Removal of copper and cadmium from the aqueous solutions by activated carbon derived from *Ceiba pentandra* hulls. *J. Hazard. Mater.*, 129 (1–3): 123–129.
12. Zhang, J.; Li, Y.; Zhang, C.; Jing, Y. (2008) Adsorption of malachite green from aqueous solution onto carbon prepared from Arundo donax root. *J. Hazard. Mater.*, 150 (3): 774–782.
13. Khattri, S.D.; Singh, M.K. (1999) Colour removal from dye wastewater using sugar cane dust as an adsorbent. *Adsorp. Sci. Technol.*, 17 (4): 269–282.
14. Papinutti, L.; Mouso, N.; Forchiassin, F. (2006) Removal and degradation of the fungicide dye malachite green from aqueous solution using the system wheat bran—*Fomes sclerodermeus*. *Enzyme Microb. Technol.*, 39 (4): 848–853.
15. Onal, Y. (2006) Kinetics of adsorption of dyes from aqueous solution using activated carbon prepared from waste apricot. *J. Hazard. Mater.*, 137 (3): 1719–1728.
16. Garg, V.K.; Kumar, R.; Gupta, R. (2004) Removal of malachite green dye from aqueous solution by adsorption using agro-industry waste: A case study of Prosopis cineraria. *Dyes Pigments*, 62 (1): 1–10.
17. Anonim. (2000) Kuru ve Sert Kabuklu Meyveler Dış Pazar Araştırması. İhracatı Geliştirme Etüd Merkezi, Ankara.
18. Ardejani, F.D.; Badii, Kh.; Limaee, N.Y.; Shafaei, S.Z.; Mirhabibi, A.R. (2008) Adsorption of Direct Red 80 dye from aqueous solution onto almond shells: Effect of pH, initial concentration and shell type. *J. Hazard. Mater.*, 151 (2–3): 730–737.
19. Bulut, Y.; Tez, Z. (2007) Adsorption studies on ground shells of hazelnut and almond. *J. Hazard. Mater.*, 149 (1): 35–41.
20. Kazemipour, M.; Ansari, M.; Tajrobehkar, S., Majdzadeh, M.; Kermani, H.R. (2008) Removal of lead, cadmium, zinc, and copper from industrial wastewater by carbon developed from walnut, hazelnut, almond, pistachio shell, and apricot stone. *J. Hazard. Mater.*, 150 (2): 322–327.
21. Rajgopal, S.; Karthikeyan, T.; Kumar, B.G.P.; Miranda, L.R. (2006) Utilization of fluidized bed reactor for the production of adsorbents in removal of malachite green. *Chem. Eng. J.*, 116 (3): 211–217.
22. Estevinho, B.N.; Ribeiro, E.; Alves, A.; Santos, L. (2008) A preliminary feasibility study for pentachlorophenol column sorption by almond shell residues. *Chem. Eng. J.*, 136 (2–3): 188–194.
23. Alkan, M.; Dogan, M.; Turhan, Y.; Demirbas, O.; Turan, P. (2008) Adsorption kinetics and mechanism of maxilon blue 5G dye on sepiolite from aqueous solutions. *Chem. Eng. J.*, 139 (2): 213–223.
24. Oliveira, L.S.; Franca, A.S.; Alves, T.M.; Rocha, S.D.F. (2008) Evaluation of untreated coffee husks as potential biosorbents for treatment of dye contaminated waters. *J. Hazard. Mater.*, 155 (3): 507–512.
25. Banat, F.; Al-Asheh, S.; Al-Makhadmeh, L. (2003) Evaluation of the use of raw and activated date pits as potential adsorbents for dye containing waters. *Process Biochem.*, 39 (2): 193–202.
26. Lagergren, S. (1898) About the theory of so-called adsorption of soluble substance. *Kung Sven. Veten. Hand*, 24: 1–39.
27. Ho, Y.S.; McKay, G. (1998) Kinetic models for the sorption of dye from aqueous solution by wood. *J. Environ. Sci. Health B*, 76 (B2): 183–191.
28. Weber, Jr. W.J.; Morriss, J.C. (1963) Kinetics of adsorption on carbon from solution. *J. Sanitary Eng. Div. Am. Soc. Civ. Eng.*, 89: 31–60.
29. Cheng, W.; Wang, S.G.; Lu, L.; Gong, W.X.; Liu, X.W.; Gao, B.Y.; Zhang, H.Y. (2008) Removal of malachite green (MG) from aqueous solutions by native and heat-treated anaerobic granular sludge. *Biochem. Eng. J.*, 39 (3): 538–546.
30. Srivastava, V.C.; Swamy, M.M.; Mall, I.D.; Prasad, B.; Mishra, I.M. (2006) Adsorptive removal of phenol by bagasse fly ash and activated carbon: Equilibrium, kinetics and thermodynamics. *Colloid Surface A*, 272 (1–2): 89–104.

31. Langmuir, I. (1918) The adsorption of gases on plane surfaces of glass, mica and platinum. *J. Am. Chem. Soc.*, 40 (9): 1361–1403.
32. Mittal, A. (2006) Adsorption kinetics of removal of a toxic dye, Malachite Green, from wastewater by using hen feathers. *J. Hazard. Mater.*, 133 (1–3): 196–202.
33. Janos, P. (2003) Sorption of basic dyes onto iron humate. *Environ. Sci. Technol.*, 37 (24): 5792–5798.
34. Tahir, S.S.; Rauf, N. (2006) Removal of a cationic dye from aqueous solutions by adsorption onto bentonite clay. *Chemosphere*, 63 (11): 1842–1848.
35. Hall, K.R.; Eagleton, L.C.; Acrivos, A.; Vermeulen, T. (1966) Pore- and solid-diffusion kinetics in fixed-bed adsorption under constant-pattern conditions. *Ind. Eng. Chem. Fundam.*, 5 (2): 212–223.
36. Freundlich, H.M.F. (1906) Über die adsorption in lösungen. *Z. Phys. Chem.*, 57 (A): 385–470.
37. Crini, G.; Peindy, H.N.; Gimbert, F.; Robert, C. (2007) Removal of C.I. basic green 4 (malachite green) from aqueous solutions by adsorption using cyclodextrin-based adsorbent: Kinetic and equilibrium studies. *Sep. Purif. Technol.*, 53 (1): 97–110.
38. Arief, V.O.; Trilestari, K.; Sunarso, J.; Indraswati, N.; Ismadji, S. (2008) Recent progress on biosorption of heavy metals from liquids using low cost biosorbents: Characterization, biosorption parameters and mechanism studies. *Clean*, 36 (12): 937–962.
39. Smith, J.M.; Van Ness, H.C. (1987) *Introduction to Chemical Engineering Thermodynamics*, 4th Ed.; McGraw-Hill: Singapore.
40. Dogan, M.; Ozdemir, Y.; Alkan, M. (2007) Adsorption kinetics and mechanism of cationic methyl violet and methylene blue dyes onto sepiolite. *Dyes Pigments*, 75 (3): 701–713.
41. Vermöhlen, K.; Lewandowski, H.; Narres, H.D.; Schwuger, M.J. (2000) Adsorption of polyelectrolytes onto oxides – the influence of ionic strength, molar mass, and Ca^{+2} ions. *Colloids Surf. A*, 163 (1): 45–53.
42. Ozdes, D.; Gundogdu, A.; Kemer, B.; Duran, C.; Senturk, H.B.; Soylak, M. (2009) Removal of Pb(II) ions from aqueous solution by a waste mud from copper mine industry: Equilibrium, kinetic and thermodynamic study. *J. Hazard. Mater.*, 166 (2–3): 1480–1487.
43. Sadhasivam, S.; Savitha, S.; Swaminathan, K. (2007) Exploitation of *Trichoderma harzianum* mycelial waste for the removal of rhodamine 6G from aqueous solution. *J. Environ. Manage.*, 85 (1): 155–161.